Structure formation features of large block-shaped samples from the copper and aluminum alloy produced by the wire-feed electron-beam additive technology

E O Knyazhev[1], A O Panfilov[1], T A Kalashnikova[2], K N Kalashnikov[2], A V Gusarova[2] and A V Chumaevskii[2]

[1]National Research Tomsk Polytechnic University, 30 Lenin Avenue, Tomsk 634050, Russian Federation
[2]Insitute of strength physics and materials science, 2/4 Akademicheskii Avenue, Tomsk 634055, Russian Federation

E-mail: zhenya4825@gmail.com

Abstract. In this work the study of the structure of samples made by the wire-feed electron-beam 3D printing from copper C11000 and aluminum alloy AA5056 was carried out. The presence of a dendritic structure typical of this method was revealed, as well as the presence of pores, cracks and other defects that occurred during printing. Mechanical properties of samples cut in the planar section are at a rather low level. The ultimate tensile strength of copper block samples varies between 165 and 187 MPa. The relative elongation of samples without pores is at 18%, but with the presence of pores it decreases sharply to 7%, while the strength is practically not decreased. The samples of alloy AA5056 demonstrate slightly higher mechanical properties: the strength is at the level of 190-192 MPa and the relative elongation is about 16-18%. In samples with defects such as large pores or discontinuities, the strength drops to almost zero.

1. Introdution

Additive technologies provide the opportunity to produce products of unusual and complex shape with the possibility of material saving required to the part production or reducing the lead time of the products by minimizing the subsequent machining. Metal products are not an exception, in this direction works are carried out, for example, on printing products from titanium [1,2], cobalt [3], steels [4,5] and other metals and alloys. The technologies of the metal additive manufacturing mainly include the ones based on the layer-by-layer deposition of the powder material on the substrate [6,7] and the feeding of wire filament directly into the molten pool [8,9,10]. One of the most high-performance 3D printing technologies are wire-based laser [8], electric arc [9] and electron-beam [10] techniques. The important factor of an additive materials production is the choice of manufacturing process parameters, as they influence the quality of the products. However, a mode selection might not influence the quality improvement of produced materials, as some defects at printing can be eliminated not completely or not eliminated at all. For some defects, even in externally defect-free samples, it is practically impossible to eliminate them by changing the process parameters of additive electron-beam technology. Samples, due to the presence of small pores and local discontinuities, may have a low strength compared to rolled sheet metal. This problem can be solved by material processing, for example, by friction stir processing.

This method allows to get rid of pores and cracks, and the structure and properties of the material depend on the processing direction and are at the level of strength properties of sheet metal [11].

The purpose of the present work is the analysis of repairable and nonrepairable defects in the large block-shaped samples made by the electron-beam 3D printing method from copper grade C11000 and aluminum alloy AA5056 as well as the conducting the mechanical testing of materials on the specimens with the presence or absence of defects.

2. Materials and methods of research

Samples were produced by the wire-feed electron-beam additive technology on a laboratory experimental equipment (figure 1). For 3D printing of samples, the copper wire of C11000 grade with 1 mm diameter, which was applied to a copper substrate with 5 mm thickness, and the wire from AA5056 aluminum alloy with 1.2 mm diameter, which was applied to a substrate from a similar alloy with 8 mm thickness were chosen. The modes of the basic samples manufacturing are given in Table 1. The modes are selected to be able to produce samples with large macrodefects and with a practically defect-free structure. The main adjustable parameter was the beam current. Changes in the beam current during printing have occurred smoothly from the maximum value on the first layers to the minimum value on the last ones. The main effect of changes in the beam current is a variation in the energy input to the material during the filament melting process and, as a result, the heat input.

The printing was carried out in a vacuum chamber on a substrate mounted on a movable water-cooled table. The electron beam was directed to the substrate to form a molten pool in which the feedstock material melted. Four large blocks were made in this way: the first from aluminum alloy AA5056 and the second from copper C11000, which were produced with macrodefects, as well as the one block each without ones.

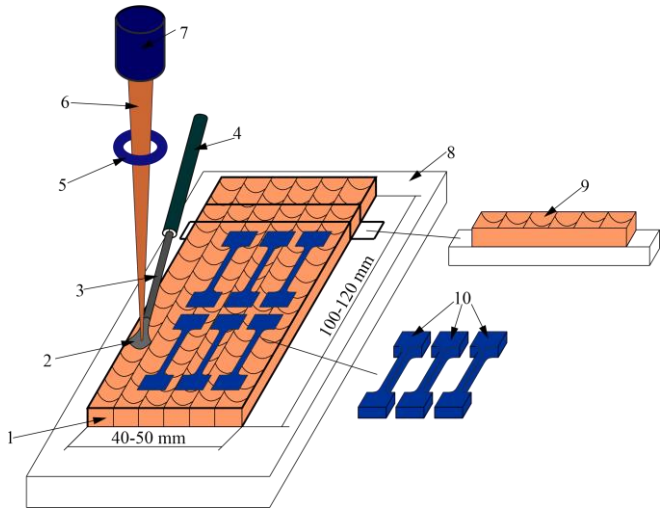

Figure 1. The scheme of the electron-beam 3D-printing (a) and cutting of specimens from the large block. 1 - block, 2 - molten pool, 3 - filament, 4 - nozzle, 5 - focusing system, 6 - electron beam, 7 - gun, 8 - substrate, 9 - cross-section metallographic specimen, 10 - test coupons for the tensile testing of the block material.

For metallographic studies of macrostructures, specimens representing cross-sections of blocks were cut out using the DK7750 electrical discharge machine (figure 1). To investigate mechanical properties of materials at the tension, test coupons were cut out, which has two shoulders and a gage section. In the presence of macrodefects, test coupons were cut out so that the gage section did not contain any irregularities of the sample macrogeometry. Before microstructural analysis, the samples were grinded and polished on diamond paste. To reveal the structure, chemical etching of samples was carried out. Metallographic examination of the samples structure was performed using confocal microscope OLYMPUS LEXT OLS4100.

Table 1. Electron-beam additive manufacturing modes for the sample production

Sample/Material	Beam current [mA] First layer/last layer	Accelerating voltage [V]	Linear printing speed [mm/min]	The presence of defects
1/5056	45/25	30	440	macrogeometry failure, large discontinuities, pores
2/5056	55/25	30	450	pores
3/C11000	40/38	30	350	pores, large discontinuities, stratification
4/C11000	50/38	30	350	pores

3. Results and discussion

Figure 2, a show the metallographic image of a copper sample (mode 3) in cross-section. The structure of the sample has a pronounced large crystalline structure caused by the directed growth of dendrites during the layer-by-layer deposition. The growth of dendrites is observed from the substrate to the upper part of the sample in the center, with the grains inclined at an angle to the substrate along the edges of blocks. The bottom part of the printed material is characterized by a fine grain structure formed before the temperature gradient leveling. It is necessary to pay attention to a large number of defects: pores (1), and stratification (2) of different sizes in the sample and on the border between the sample and the substrate. This is caused by the excessive cooling rate of the molten metal when the substrate is not sufficiently heated. In the upper part of the sample, an almost spherical pore formation (3) is noted due to evaporation of the metal from the molten pool and rapid subsequent cooling.

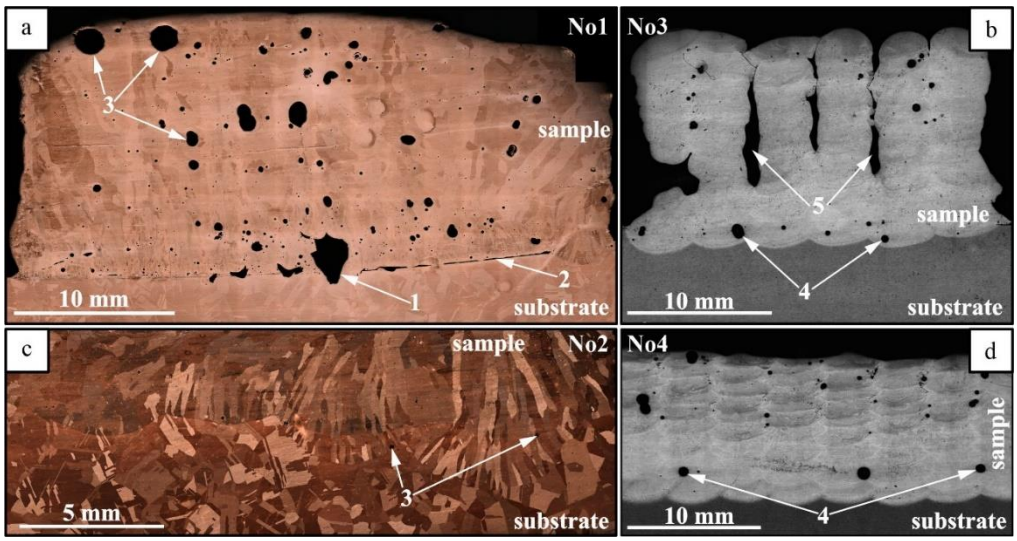

Figure 2. The cross-section of defective areas of large blocks with the presence of macrodefects in copper C11000 (a) and aluminum alloy AA5056 (b), and samples of large blocks of corresponding alloys without macrodefects (c,d), obtained by electron beam additive method.

The structure of an aluminium sample (mode 1) differs from that of a copper one both in terms of types and number of macro- and microdefects, as well as in the macrostructure determined by regularities of the material solidification during printing (figure 2, b). The figure 2, b shows a sample with a significant deviation of the printing process parameters from optimal values. The entire structure of the copper sample is saturated with grains formed by the dendrite growth during printing, while in the aluminum sample the structure appears more in the separation into certain layers formed during

printing. The pores of different sizes are also present in the sample (4). The sample is characterized by a printing failure which causes the sample volume to be unfilled (5), due to the poor flowing of the material as a result of a process failure, leading to the growth of individual vertical "walls" in the middle part of the block.

In copoper samples without large macrodefects and discontinuities, produced by the mode 4, there is the formation of large columnar grains from the substrate, without the formation of defects at the border (figure 2, c). The increased beam current in the lower layers led to a better fusion of the individual layers with each other and with the substrate. The sample contains pores (3), but in significantly smaller quantities. In the boundary zone, the sample fusion area with the substrate and the grain growth perpendicular to the edge of the molten pool during printing are clearly distinguished.

In aluminum alloy 5556 samples produced by the mode 2, there are no failures of the macrogeometry (figure 2, d). There are no large discontinuities due to the more intense melting of the filament due to a higher beam current. However, the pore formation (4) in the material cannot be completely eliminated.

Tensile tests on the aluminum alloy sample material show that the mechanical properties after additive printing of samples in the shape of large blocks are at a sufficiently low level (figure 3, a). The ultimate tensile strength of the test coupons is on average 190-192 MPa, the ductility is about 16-18%. For this alloy such values are extremely low. The test diagrams are characterized by two plastic stages of the strain hardening, and one elastic stage (figure 3, a). Once the yield strength is reached, strain passes to the parabolic stage of the plastic flow (with a variable parabolic hardening coefficient), with a clearly visible jump-shaped change in load force due to the Portevin - Le Chatelier effect. In the last stage, there is a transition to the last stage of deformation with the formation of the "neck" and subsequent fracture of samples.

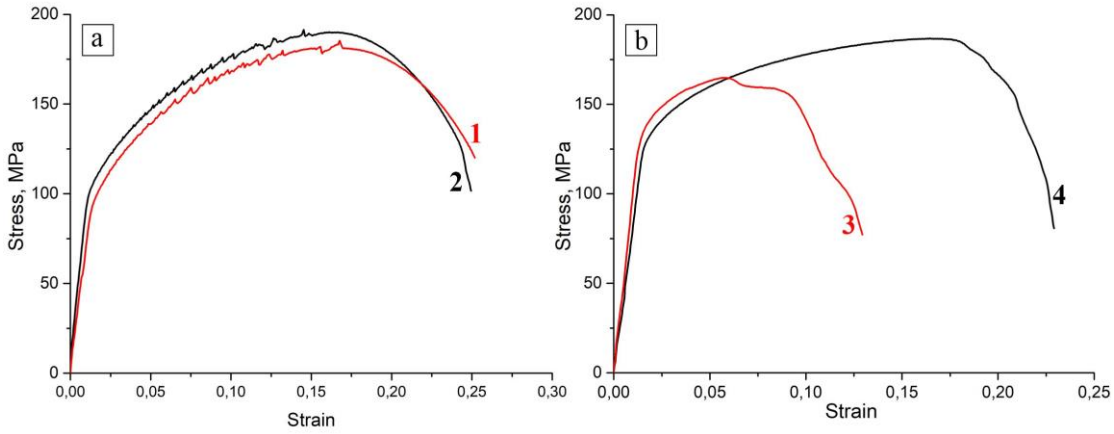

Figure 3. Test diagrams of aluminium alloy AA5056 (a) and copper C11000 (b) samples after the electron-beam printing. The curves correspond to the mode numbering.

Mechanical properties of the C11000 grade copper also show quite low material characteristics (figure 3, b), which drop sharply if the material has defects in the coupons, such as pores or stratification. At small changes in the strength of highly defective and less defective coupons from 165 to 187 MPa, relative elongation in defective ones sharply decreases from 18 to 7%. It should be noted that both graphs are characterized by a general tendency of rather sharp transition to the stage of "neck" formation. The deformation in these samples also occurs in one elastic stage and two plastic deformation stages. The final stage of plastic deformation consists in the formation of the neck with subsequent fracture of the sample. For both samples, the stage with a high constant strain-hardening factor is almost absent, partly due to the fact that the neck formation stage with subsequent fracture begins almost immediately after the parabolic stage as a result of small pores in the coupon material, while larger defects cause the fracture almost immediately after the transition to the plastic flow stage.

4. Conclusions

Carried out researches show that in the samples produced by the wire-feed electron-beam additive technology, the defects of different structural-scale level are formed. At the same time, the formation of defects of the same type, for example, large discontinuities in aluminum alloys, can be avoided by adjusting the printing process parameters. The increase in the heat input during printing of both copper and aluminum samples leads to an increase in the flowability of the molten pool material, which contributes to a longer life-time of the metal in the liquid state and reduces the possibility of the large discontinuities and macrodefects formation. The formation of defects as pores in the structure of copper or aluminum alloy is almost impossible to avoid completely, which leads to low strength properties of both copper C11000 (165-187 MPa) and AA5056 alloy (190-192 MPa). Therefore, the use of post-treatment to remove pores after printing and harden the additive products, for example, friction stir processing, is promising.

Acknowledgment

The work on the study of the additive electron-beam printing parameters was performed according to the Government research assignment for ISPMS SB RAS, project No. III.23.2.11. Works on producing and studying the structure and properties of samples in the shape of blocks from aluminum alloy AA5056 and copper C11000 were performed within the framework of the RSF project 19-79-00136.

References

[1] Wang X and Chou K 2018 Effect of support structures on Ti-6Al-4V overhang parts fabricated by powder bed fusion electron beam additive manufacturing *J. of Materials Processing Technology* **257** pp 65-78

[2] Sahoo S and Chou K 2016 Phase-field simulation of microstructure evolution of Ti–6Al–4V in electron beam additive manufacturing process *Additive Manufacturing* **9** pp 14-24

[3] Almanza E, Perez M et al 2017 Corrosion resistance of Ti-6Al-4V and ASTM F75 alloys processed by electron beam melting *Journal of Materials Research and Technology* **6** Iss.3 pp 251-257

[4] Wanjara P, Brocju M et al 2007 Electron beam freeform of stainless steel using solid wire feed *Materials and Design* **28** pp 2278-2286

[5] Koptyug A et all 2020 Compositionally-tailored steel-based materials manufactured by electron beam melting using blended pre-alloyed powders *Materials Science and Engineering:* A **771** p 11

[6] Majeed A, Ahmed A et al 2019 Surface quality improvement by parameters analysis, optimization and heat treatment of AlSi10Mg parts manufactured by SLM additive manufacturing *International Journal of Lightweight Materials and Manufactur*e **2** iss.4 pp 288-295

[7] Aboutaleba A, Mahtabib M et al 2019 Multi-objective accelerated process optimization of mechanical properties in laser-based additive manufacturing: Case study on Selective Laser Melting (SLM) Ti-6Al-4V *Journal of Manufacturing Processes* **38** pp 432-444

[8] Ding X, Li H et al 2017 Application of infrared thermography for laser metal-wire additive manufacturing in vacuum *Infrared Physics & Technology* **81** pp 166-169

[9] Sun R, Li L et al 2018 Microstructure, residual stress and tensile properties control of wire-arc additive manufactured 2319 aluminum alloy with laser shockpeening *J. of Alloys and Compounds* **747** pp 255-265

[10] Shu X, Chen G et al 2018 Microstructure evolution of copper/steel gradient deposition prepared using electron beam freeform fabrication *Materials Letters* **213** pp 374-377

[11] Lashgari H, Kong C et al 2018 The effect of friction stir processing (FSP) on the microstructure,nanomechanical and corrosion properties of low carbon $CoCr_{28}Mo_5$ alloy *Surface & Coatings Technology* **354** pp 390-404